Slow Light Augmented Unbalanced Interferometry for Extreme Enhancement in Sensitivity of Measuring Frequency Shift in a Laser

Ruoxi Zhu^{1,*}, Zifan Zhou¹, Jinyang Li², Jason Bonacum³, David D. Smith⁴, and Selim M. Shahriar^{1,2,3}

¹Department of Electrical and Computer Engineering, Northwestern University, Evanston, IL 60208, USA

²Department of Physics and Astronomy, Northwestern University, Evanston, IL 60208, USA

³Digital Optics Technologies, Rolling Meadows, IL 60008, USA

⁴NASA Marshall Space Flight Center

*Email: ruoxizhu2024@u.northwestern.edu

Abstract

We demonstrate a slow-light augmented unbalanced Mach-Zehnder interferometer (MZI) which can be used to enhance very significantly the sensitivity of measuring the frequency shift in a laser. The degree of enhancement depends on the group index of the slow-light medium, the degree of imbalance between the physical lengths of the two arms of the MZI, and the spectral width of the laser. For a laser based on a high-finesse cavity, yielding a narrow quantum noise limited spectral width, the group index has to be larger than the finesse in order to achieve enhancement in measurement sensitivity. For the reported results, strong slow-light effect is produced by employing electro-magnetically induced transparency via coherent population trapping in a buffergas loaded vapor cell of Rb atoms, with a maximum group index of ~1759. The observed enhancement in sensitivity for a range of group indices agrees well with the theoretical model. The maximum enhancement factor observed is ~22355, and much larger values can be obtained using cold atoms for producing the slow-light effect, for example. The sensitivity of any sensor that relies on measuring the frequency shift of a laser can be enhanced substantially using this technique. These include, but are not limited to, gyroscopes and accelerometers based on a conventional ring laser or a superluminal ring laser, and detectors for virialized ultra-light field dark matter. We also show how similar enhancements can be achieved in a slow-light augmented unbalanced Michelson interferometer.

1. Introduction

Many sensors rely on determining measurands based on shifts in frequencies of lasers. These include, but are not limited to, gyroscopes and accelerometers based on a conventional ring laser [1,2] or a superluminal ring laser [3], and detectors for virialized ultra-light field dark [4]. To achieve better precision in measuring frequency shifts, our group has proposed several schemes employing superluminal lasers, which is a type of laser where the group velocity of light exceeds the speed of light in the vacuum [3,5,6,7,8,9, 10,11,12,13,14,15,16]. However, it turns out that it may be possible to achieve a sensitivity enhancement with a slow-light augmented unbalanced Mach-Zehnder Interferometer (SLAUMZI). The idea is closely related to what Boyd et al. has showed, where the use of slow-light medium inside an unbalanced Mach-Zehnder Interferometer amplifies the frequency sensitivity [17]. However, their work did not take into account the spectral width of the laser, and how that affects the measurement of frequency shift. Therefore, by considering the finite linewidth of a laser, we present the concept of improving sensitivity with SLAUMZI and analyze the minimum measurable frequency shift in a SLAUMZI. Furthermore, we present experimental results demonstrating such an enhancement, in close agreement with the theoretical model. The rest of the paper is organized as follows. In Section 2, we present the theoretical model for enhancing sensitivity of measuring frequency shifts using a SLAUMZI. In Section 3, we present the experimental results for realizing a SLAUMZI and using it to demonstrate enhancement in frequency shift measurement sensitivity. Concluding remarks are presented in Section 4.

2. Theory

The concept of slow-light augmented unbalanced interferometry (SLAUI) for the purpose of enhancing the sensitivity in measuring frequency shift in a source can be realized using several different configurations. These include, for example, a Mach-Zehnder Interferometer (MZI) or a Michelson Interferometer (MI), as illustrated schematically in Figure 1. Consider first the case of an unbalanced MZI, as shown in Figure 1(a). Here, we denote the length of the upper arm as L_1 ,

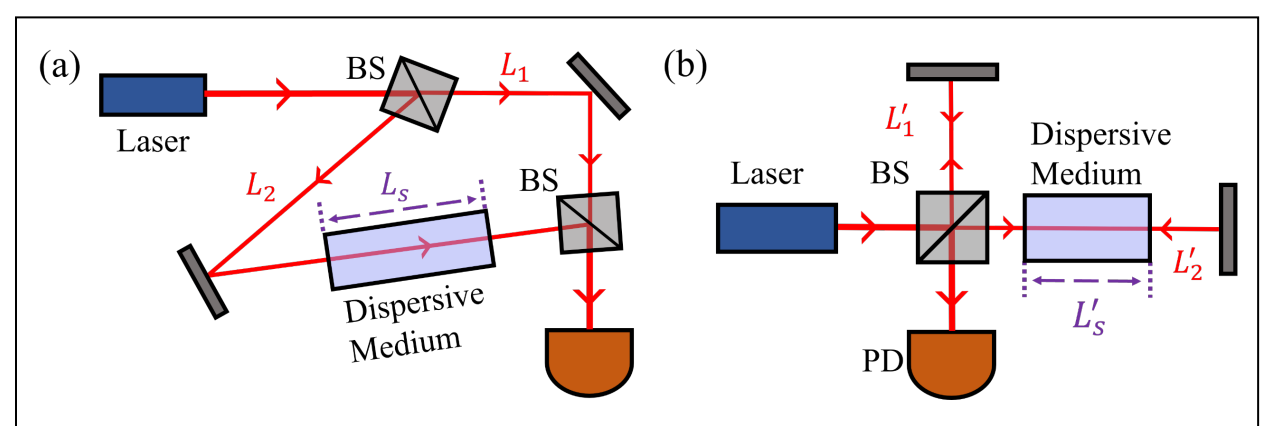


Figure 1. Illustration of sensitivity-enhanced interferometers using (a). Mach-Zehnder interferometers and (b). Michelson Interferometers.

and the length of the lower arm as L_2 , which can be expressed as $L_2 = L_1 + L_0 + L_s$, where L_s is the length of the slow-light medium and L_0 is the intrinsic path-length difference. We denote the frequency as ω , and the refractive index experienced by the laser field in the slow-light medium as $n(\omega)$. The phase difference between the two paths can be expressed as:

$$\Phi(\omega) = L_0 \omega / c_0 + n(\omega) L_s \omega / c_0, \tag{1}$$

where c_0 is the vacuum speed of light. Therefore, the variation in the phase difference due to a change in the frequency can be expressed as:

$$\frac{d\Phi}{d\omega} = \frac{L_0}{c_0} + \frac{L_s}{c_0} n_g \,, \tag{2}$$

where n_g is the group index experienced by the laser at frequency ω . We denote as the reference point the condition when the slow-light medium is replaced by vacuum, corresponding to unity group index (i.e., $n_g = 1$). In what follows, we will refer to the condition of $n_g > 1$ as the slow-light case, and the condition of $n_g = 1$ as the vacuum case. The fringe magnification factor, denoted as M, is then defined as the ratio between the phase difference variation in the slow-light case and the same for the vacuum case:

$$M = \frac{\left(d\Phi / d\omega\right)_{SL}}{\left(d\Phi / d\omega\right)_{VAC}} = \frac{L_0 / c_0 + n_g L_s / c_0}{L_0 / c_0 + L_s / c_0} = \frac{\tau_0 + n_g \tau_D}{\tau_0 + \tau_D} = \frac{\tau_{SL}}{\tau_{VAC}},$$
(3)

where
$$\tau_0 \equiv L_0/c_0$$
, $\tau_D \equiv L_S/c_0$, $\tau_{SL} \equiv \tau_0 + n_g \tau_D$, and $\tau_{VAC} \equiv \tau_0 + \tau_D$.

We assume the signal at the detection port is maximum when the phase difference between the two arms has a null value, and denote it as S_0 . The signal as a function of the phase difference then can be expressed as $S_0 \cos^2 \Phi(\omega)$. We define as ω_0 the frequency at which the group index is evaluated, and denote as $\Delta \omega$ the deviation away from this frequency (i.e., $\Delta \omega \equiv \omega - \omega_0$). The signal then can be expressed as:

$$S = S_0 \cos^2[\Phi(\omega_0) + \frac{L_0}{c_0} \Delta\omega + \frac{L_s}{c_0} n_g \Delta\omega]$$

$$= S_0 \cos^2[\Phi(\omega_0) + \tau_0 \Delta\omega + \tau_D n_g \Delta\omega] = S_0 \cos^2[\Phi(\omega_0) + \tau_{SL} \Delta\omega]$$
(4)

The findings of the analyses in the rest of the paper remain valid for an arbitrary value of the phase offset, $\Phi(\omega_0)$. As such, for notational clarity but without loss of generality, we set the value of $\Phi(\omega_0)$ to zero, so that:

$$S = S_0 \cos^2(\tau_{SL} \Delta \omega) \,. \tag{5}$$

Equation (5) applies to the situation where the laser linewidth is assumed to be zero. Of course, in practice, the laser will have a finite linewidth, greater than or equal to its quantum noise limited value known as the Schawlow-Townes Linewidth (STL). We consider first the limiting case where the linewidth equals the STL, which can be expressed as follows [18,19,20,21,2]:

$$\Gamma_{STL} = \frac{\hbar \omega \gamma_c^2}{2P_0} \equiv \frac{1}{\tau_{STL}},\tag{6}$$

where P_0 is the laser output power, and γ_c is the cavity linewidth, given by the inverse of the cavity decay time, τ_c . Here we also define τ_{STL} as the coherence time of the laser. The STL results from the loss of coherence due to spontaneous emission, and can be derived using many different ways, including the master equations approach, the Langevin noise operator approach, and the random walk approach [19,22], all yielding essentially the same result. Here, we consider the model employing the random walk approach, and limit our consideration to the case where the laser operates at the peak of the gain spectrum, so that the so-called Henry factor [19] can be ignored, noting that the analysis that follows can be easily extended to the more general case where the Henry factor is dominant. In this model, spontaneous emission events cause random phase jumps. The probability of such jumps is assumed to follow a Gaussian distribution. Taking into account the phase jitter resulting from the spontaneous emission events, the signal received by the photodetector in the SLAUMZI can be expressed as:

$$S = S_0 \cos^2(\tau_{SL} \Delta \omega + \phi_2 - \phi_1)$$

$$= \frac{S_0}{2} + \frac{S_0}{2} \left[\cos(2\tau_{SL} \Delta \omega) \cos(2\Delta \phi) - \sin(2\tau_{SL} \Delta \omega) \sin(2\Delta \phi) \right], \tag{7}$$

where $\Delta \phi = \phi_2 - \phi_1$ and $\phi_{1(2)}$ is the random phase of the upper(lower) arm at the combining beam splitter. Therefore, the two instances when the laser phase jumps to ϕ_1 and ϕ_2 are separated by the time difference τ_{VAC} . The probability of having two instances of phase jumps separated by τ_{VAC} can thus be expressed as [22]:

$$f(\Delta \phi_{\tau_{VAC}}) = \frac{1}{\sqrt{2\pi \tau_{VAC}/\tau_{STL}}} \exp(-\frac{\Delta \phi_{\tau_{VAC}}^2}{2(\tau_{VAC}/\tau_{STL})}). \tag{8}$$

Therefore, the output power can be expressed as:

$$S = \frac{S_0}{2} + \frac{S_0}{2} \left[\cos(2\tau_{SL}\Delta\omega) \left\langle \cos(2\Delta\phi_{\tau_{VAC}}) \right\rangle - \sin(2\tau_{SL}\Delta\omega) \left\langle \sin(2\Delta\phi_{\tau_{VAC}}) \right\rangle \right]. \tag{9}$$

The expectation value $\langle \cos(2\Delta\phi_{\tau_{VAC}}) \rangle$ can be calculated as:

$$\int_{-\infty}^{+\infty} \cos(2\Delta\phi_{\tau_{VAC}}) f(\Delta\phi_{\tau_{VAC}}) d(\Delta\phi_{\tau_{VAC}}) = \frac{1}{2} e^{-1/4} \exp(-\frac{\tau_{VAC}}{2\tau_{STL}}). \tag{10}$$

It is obvious that $\langle \sin(2\Delta\phi_{\tau_{VAC}})\rangle = 0$ because of the symmetry around the origin. Therefore, the output power is:

$$S = \frac{S_0}{2} + \frac{S_0}{4} e^{-1/4} \exp(-\frac{\tau_{VAC}}{2\tau_{CT}}) \cos(2\tau_{SL}\Delta\omega). \tag{11}$$

Thus, the contrast is decreased as the length imbalance increases, which is consistent with the result that interference signal disappears when the time delay greatly exceeds the coherence time.

For potential applications, it is important to determine the minimum measurable frequency shift (MMFS) in the SLAUMZI and compare it with the MMFS for the conventional approach [2,23], which is limited by the laser linewidth and measurement time. The MMFS for the SLAUMZI is given by the uncertainty in the observed value of the laser frequency, expressed as:

$$\delta\omega_{SLAUMZI} = \left| \frac{\Delta S}{\partial S/\partial \omega} \right|. \tag{12}$$

where ΔS is the standard deviation of the signal, accounting for all sources of noise. We define N as the number of photons per second received by a photodetector corresponding to the peak signal S_0 , and τ_M as the measurement time. We assume that the intrinsic length (i.e., $L_0 + L_s$) in the SLAUMZI is restricted to be less than a meter, so that the value of τ_{VAC} is less than 3.3 nsec. Consider next the typical value of τ_{STL} . For a ring laser with a length of 70 cm, output coupled intensity reflectivity of 0.5, and an output power of 400 μW , which does not experience additional broadening due to the Henry factor[19], has an STL of ~0.56 Hz [24]. If the laser is shorter by a factor of 10^3 , which would be typical for a diode laser, the value of STL would be larger by a factor of 10^6 , yielding a value of 560 kHz. The Henry factor, which is highly relevant for a diode laser, is typically of the order of 50 [19], which would make the value of STL to be ~ 28 MHz. Modern diode lasers, however, has a much larger output power. If we assume an output power of 40 mW, then the STL would be 280 kHz (which is close to the value of the measured linewidth of the laser we have used as the source for the SLAUMZI). The value of τ_{STL} for such a laser would be ~3.6 μ sec. As such, it is reasonable to make the approximation that $\tau_{VAC} \ll \tau_{STL}$.

The ideal method for measuring any shift in the frequency of the laser would make use of the so-called hopping method [25], which would work as follows for the SLAUMZI. The frequency of the laser would be modulated with a square wave, thus making it jump by a value of $\Delta \omega = \pm (\pi / \tau_{SL})$, and the signal observed at these two extrema (corresponding to maximum slopes) would be subtracted from one another. If the unmodulated value of the laser frequency corresponds to the peak of the signal, for example, then the subtracted signal would be zero, in the absence of any noise. Any deviation of the subtracted signal away from zero would then represent a shift in the laser frequency. It can be shown that the minimum frequency uncertainty obtained using this hopping method is the same as what one would obtain if the signal is measured at the point where

it has the highest slope [25]. As such, in what follows, we determine the value of $\delta\omega_{SLAUMZI}$ at one of these points, corresponding to a bias frequency shift of $\Delta\omega = \pi/(2\tau_{SL})$.

We assume that the experiment is limited by quantum noise only. In that case, the variance of the signal is due simply to the shot noise, which dictates that the uncertainty in number of photons detected equals the square-root thereof. Assuming ideal detection efficiency, we then get that for a bias frequency shift of $\Delta\omega = \pi/(2\tau_{SL})$ the minimum uncertainty in the laser frequency is then given by:

$$\delta\omega_{SLAUMZI} = \frac{\sqrt{2N\tau_M}}{e^{1/4}N\tau_M\tau_{SL}\exp[-\tau_{VAC}/(2\tau_{STL})]}.$$
 (13)

Since $\tau_{VAC} \ll \tau_{STL}$, this equation simplifies to:

$$\delta\omega_{SLAUMZI} \approx \frac{\sqrt{2}}{e^{1/4}\tau_{SL}[1 - \tau_{VAC} / (2\tau_{STL})]\sqrt{N\tau_M}} \approx \frac{\sqrt{2}}{e^{1/4}\tau_{SL}\sqrt{N\tau_M}}.$$
 (14)

If we denote by η the quantum efficiency of the detector, and by σ the attenuation of the signal [26,27,28], then the equation becomes:

$$\delta\omega_{SLAUMZI} \approx \frac{\sqrt{2}}{e^{1/4}\tau_{SL}\sqrt{\eta\sigma N\tau_{M}}}$$
 (15)

To compare this sensitivity with what can be achieved using the conventional approach, we consider the standard technique whereby the frequency of the laser is measured by beating it with a reference laser which has a much narrower STL (delta function limit). A closely related technique is used, for example, in a He-Ne ring laser gyroscope [2,23]. In that case, the laser in one direction beats with the laser in the other direction. Assuming full suppression of common mode noise, the observed uncertainty is then the sum of the uncertainties in the frequency of the laser in each direction, which in turn determines the uncertainty in the measured rotation rate. Under quantum noise limited operation, it can be shown [2] that the spectral uncertainty in such a measurement is given by twice the geometric mean of the STL of each laser and the measurement bandwidth. In the case we are considering, where the STL of the reference laser is vanishingly small, it would then follow that the spectral uncertainty in the measurement of the test laser is given by the geometric mean of the STL of the test laser and the measurement bandwidth. Assuming the same values of τ_M and N and using the notation introduced above, while taking into account the finite quantum efficiency of the detector, we can write the MMFS for the standard technique as:

$$\delta\omega_{STD} = \sqrt{\frac{\gamma_{STL}}{\eta \tau_{M}}} = \sqrt{\frac{\gamma_{c}^{2}}{2\eta N \tau_{M}}} = \frac{1}{\tau_{c} \sqrt{2\eta N \tau_{M}}}.$$
 (16)

Thus, the ratio between the MMFSs of the SLAUMZI and that of the standard technique is:

$$\frac{\delta\omega_{SLAUMZI}}{\delta\omega_{STD}} = \frac{2\tau_c}{e^{1/4}\tau_{SL}} \sim 1.6 \frac{\tau_c}{\sqrt{\sigma}\tau_{SL}}.$$
 (17)

Equation (17) can be expressed in terms of the length scales as:

$$\frac{\delta\omega_{SLAUMZI}}{\delta\omega_{STD}} = \frac{2F\tau_{RT}}{e^{1/4}(\tau_0 + n_g\tau_D)\sqrt{\sigma}} = \frac{2FL_c}{e^{1/4}(L_0 + n_gL_D)\sqrt{\sigma}},$$
(18)

where F is the cavity finesse and $L_c = c_0 \tau_{RT}$ is the cavity length for the laser. In the limit where $n_g L_D \gg L_0$ and the cavity length equals the length of the dispersive media, we can approximate the ratio to:

$$\frac{\delta\omega_{SLAUMZI}}{\delta\omega_{Beat}} \sim 1.6 \frac{F}{n_{s}\sqrt{\sigma}}.$$
 (19)

Thus, in order to achieve a smaller MMFS than what can be obtained with the conventional technique, the group index in an SLAUMZI must be larger than 1.6 times the finesse of the laser, in the ideal limit of $\sigma \to 1$. In a typical He-Ne Ring Laser Gyro, the finesse is on the order of 10^4 . Thus, a slow light with a group index of 10^7 , for example, would increase the measurement accuracy for rotating sensing by nearly three orders of magnitude. Of course, if a superluminal laser is used for rotation sensing, this enhancement would be above the factor of enhancement achievable using the superluminal laser alone, assuming that the STL of a superluminal laser remains essentially the same as that of a conventional laser with identical operating parameters, such as the cavity length, cavity finesse, and the output power [6].

The results we have presented above show that, for proper choice of parameters, the SLAUMZI may be used to enhance the sensitivity of any sensor where the measurand of interest is proportional to the shift in the frequency of a laser. One device that falls in this category is an active ring laser gyroscope. In principle, the rotation rate can be inferred simply from the shift in the frequency of a unidirectional ring laser. The approach for determining the rate of rotation via measurements of shifts in the frequencies of two counter-propagating lasers is discussed later. One issue of concern for rotation sensing using this approach is that the SLAUMZI itself experiences Sagnac effect in the phase difference between two arms. This problem can be overcome by making use of a "figure 8" type configuration for the SLAUMZI, so that the net enclosed area is zero. Alternatively, one can use a slow-light augmented unbalanced Michelson Interferometer (SLAUMI). Figure 1(b) shows a possible configuration of the SLAUMI. Just as in the case of the SLAUMZI, it is necessary to have an imbalance in the lengths of the two arms. Here, L'_1 is defined as twice the distance between the beam splitter and the mirror at the end of path 1. Similarly, L'_2 is defined as twice the distance between the beam splitter and the mirror at the end of path 2. These two lengths are related as follows: $L'_2 = L'_1 + L'_0 + L'_S$. Note that this means that L'_S is twice the physical length of the slow-light medium. Similarly, L_0' is twice the difference between $L_2'/2$

and $L'_1/2$ when the length of the slow-light medium is zero. Thus, results similar to the case of the SLAUMZI can be obtained by simply substituting L_s by L'_s and L_0 by L'_0 in Eq. (1). As such, the enhancement factor can be expressed as:

$$M = \frac{L'_0 / c_0 + n_g L'_s / c_0}{L'_0 / c_0 + L'_s / c_0} = \frac{\tau'_0 + n_g \tau'_D}{\tau'_0 + \tau'_D} \equiv \frac{\tau'_{SL}}{\tau'_{VAC}}.$$
 (20)

The ratio between the MMFS for the SLAUMI and the standard approach can be then expressed as:

$$\frac{\delta\omega_{SLAUMI}}{\delta\omega_{STD}} = \frac{2\tau_c}{e^{1/4}\sqrt{\sigma}\tau_{SL}'} \sim 1.6\frac{\tau_c}{\sqrt{\sigma}\tau_{SL}'}.$$
 (21)

where $\tau'_{SL} = \left(L'_0 + n_g L'_S\right)/c_0$. We note that it is also possible to realize a slow-light enhanced Fabry-Perot resonator, for which one must take into account effects of multiple interference among the laser beams generated during multiple bounces off the mirrors. The analysis for such a case is more involved, and will be presented in a future paper.

It is noteworthy that even though the analysis of the MMFS is conducted by assuming the laser linewidth is quantum noise limited, there is no fundamental requirement for making such an assumption. In fact, for any laser that has a finite linewidth Γ_L , we can define the following quantity:

$$\tau_L \equiv \frac{1}{\Gamma_L}.\tag{22}$$

The behavior of such a laser can also be modeled as originating from random phase jumps. Here, for simplicity, we assume the phase jumps will have a Gaussian probability distribution (in general, it would necessary to characterize the noise processes carefully to determine the nature of the probability distribution.) As such, the steps shown in eqns. (7) through (11) would apply in this case. For such a laser, the MMFS for the standard technique can be expressed simply as:

$$\delta\omega_{STD} = \frac{1}{\sqrt{\eta \tau_L \tau_M}} \,. \tag{23}$$

Therefore, with such a laser, the ratio between the MMFS for the SLAUMZI and the standard technique becomes:

$$\frac{\delta\omega_{SLAUMZI}}{\delta\omega_{STD}} = \frac{\sqrt{2}/\left(e^{1/4}\tau_{SL}\sqrt{\sigma N\tau_{M}}\right)}{1/\sqrt{\tau_{L}\tau_{M}}} = \frac{1}{e^{1/4}\tau_{SL}}\sqrt{\frac{2\tau_{L}}{\sigma N}}.$$
 (24)

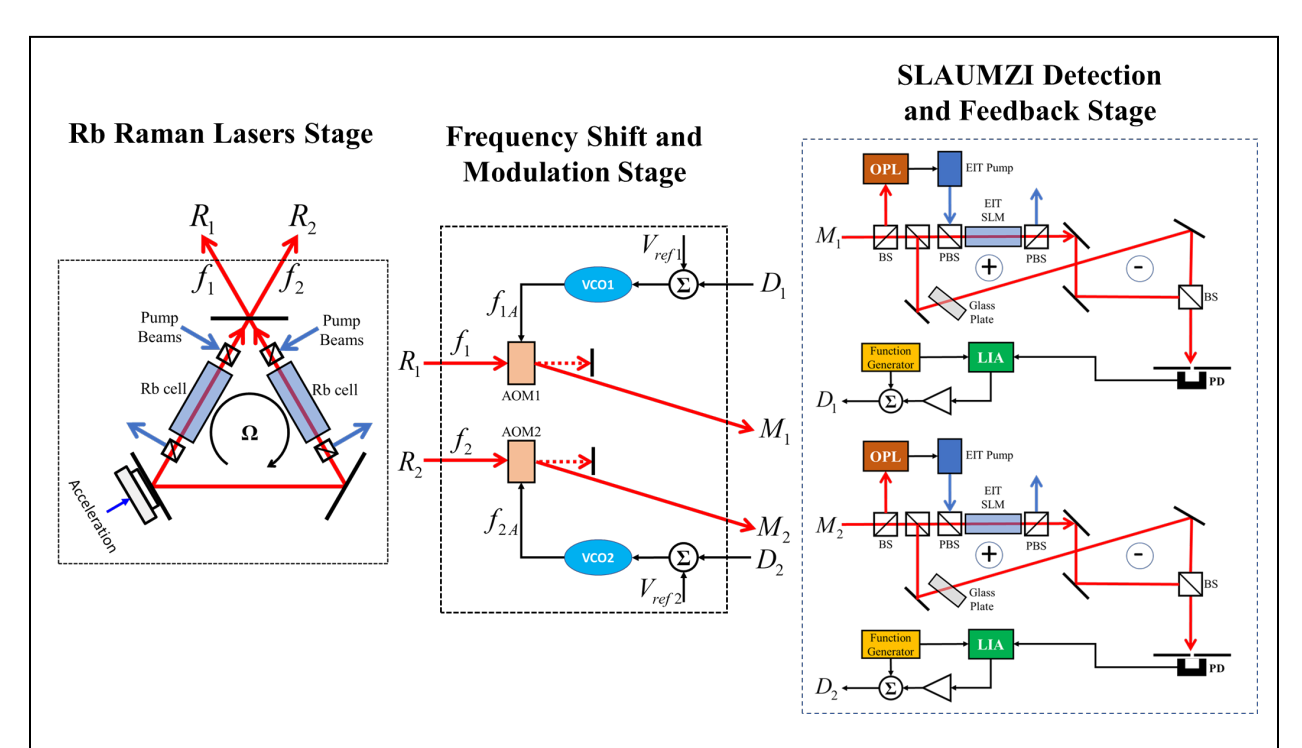


Figure 2. The schematic of an accelerometer-incorporated slow-light enhanced gyroscope used for rotation sensing and accelerometry. The details are explained in the text. Note that each MZI is configured in the "figure 8" shape to eliminate the Sagnac effect.

Fig.2 shows a configuration for a SLAUMZI enhanced gyroscope and accelerometer. The left panel shows a pair of bi-directional Raman lasers, which can be either subluminal or superluminal, employing gain from two separate cells, without any cross-talks. In order to take advantage of the SLAUMZI technique, it is necessary to employ a slow-light medium with a very large group index. One approach for achieving a group index as large as ten million is to make use of the process of electro-magnetically-induced transparency (EIT) in a Λ system [29,30]. For such a process, both legs of the beams have to be resonant with respect to the intermediate state. On the other hand, a Raman laser is always detuned by nearly a GHz away from any excited state. As such, in order to realize the EIT process, it is necessary to shift the Raman laser output with an acousto-optic modulator (AOM), for example, so that the shifted beam becomes resonant with one leg of the Λ system. In addition, it is necessary to ensure that the optical fields are phase coherent, even though they would differ in frequency by the ground state splitting. To fulfill this requirement, it is necessary to make use of another laser for the second leg, and off-set phase lock it to the Raman laser.

There are two laser outputs R_1 and R_2 through the output coupler. Assume the lasing frequencies of these two laser outputs are f_1 and f_2 . Consider first one of the outputs, for example, R_1 . This is passed through an acoustic optical modulator (AOM) and is diffracted as M_1 with a frequency shift, which is denoted as f_{1A} and is determined by the voltage reference V_{ref1} in the voltage controlled oscillator (VCO). The diffracted beam M_1 will have the frequency at which the EIT effect can be produced. Before being guided to MZI, a pump laser is phase locked to M_1 using

an offset phase lock (OPL), where the offset is the hyperfine splitting between two ground states in 85 Rb atoms, i.e. 3.0357GHz. To keep the fringe at its peak intensity, a square-wave modulation is applied to the AOM along with V_{refl} and the output of the lock-in amplifier (LIA), denoted as V_{FB1} . For the other output R_2 , the same procedure is followed, using another SLAUMZI system. Without any rotations, the lock-in amplifier outputs for both R_1 and R_2 are zero. However, when the system starts to rotate, the frequencies of the output lasers will deviate from the original value with opposite signs due to the Sagnac effect, which makes V_{FB1} and V_{FB2} non-zero. Therefore, the rotation rate can be inferred from the summation of the two feedback voltages. For the case where there is only acceleration, the frequency shift in both ring laser outputs are at the same amount and direction, which makes reading from one of the feedback voltages enough to determine the acceleration. If the goal is only to measure rotation, then making use of the summation of V_{FB1} and V_{FB2} makes it possible to suppress common-mode frequency fluctuations in the gyroscope.

In the design of such a device, the frequencies of the two Raman lasers can be non-degenerate, differing in frequency by one free spectral range (FSR) of the cavity. This will eliminate the so-called lock-in effect that occurs in a ring laser gyroscope [2], which keeps the two frequencies identical until a sufficiently large rotation occurs. Cumbersome techniques such as mechanical dithering is used to eliminate this effect in a HeNe ring laser gyroscope. Use of the non-degeneracy can eliminate the need for such techniques. The non-degeneracy of the two Raman lasers is illustrated schematically in Figure 3, which corresponds to the left panel in Figure 2.

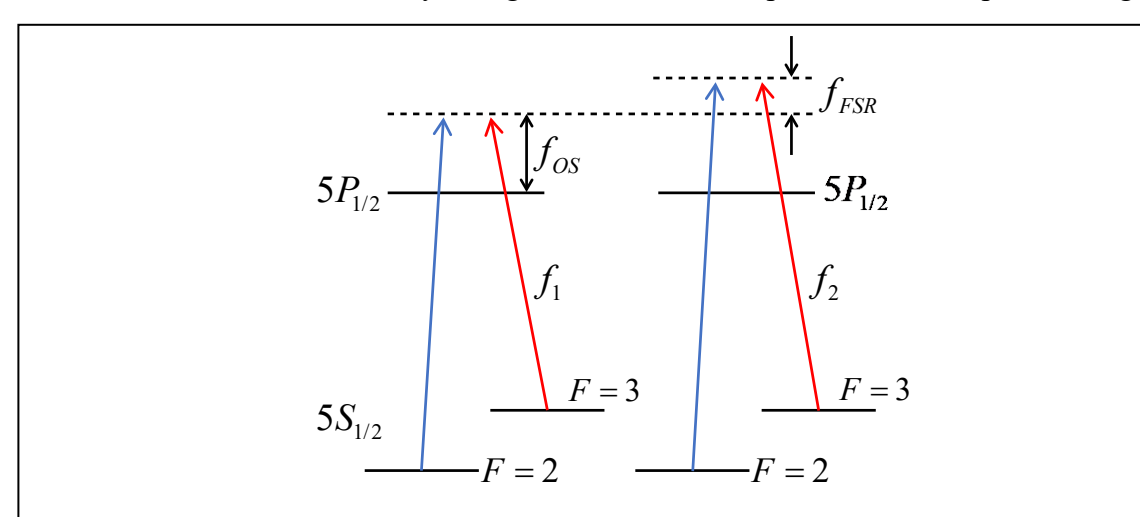


Figure 3. Schematic of relevant energy levels and the laser fields for the ring laser stage. The optical pumps are not shown in the figure, but they create population inversion between the two ground states by coupling the $5S_{1/2}$, F=3 to $5P_{3/2}$ transition.

It should be noted that the Raman laser behaves as a subluminal laser [24], which suppresses the sensitivity by the factor of the group index inside the Raman laser. However, according to the theoretical model developed by Henry [19], the STL is reduced by a factor of the square of the group index. For a conventional measurement process, we recall that the MMFS is proportional to the square root of the STL. Thus, the MMFS decreases by a factor of the group index. As such, if Henry's model holds true, then the net frequency sensitivity of Raman laser under conventional detection will be unaffected by the group index inside the Raman laser. An extension of our analysis for the MMFS for the SLAUMZI shows that the group index inside the

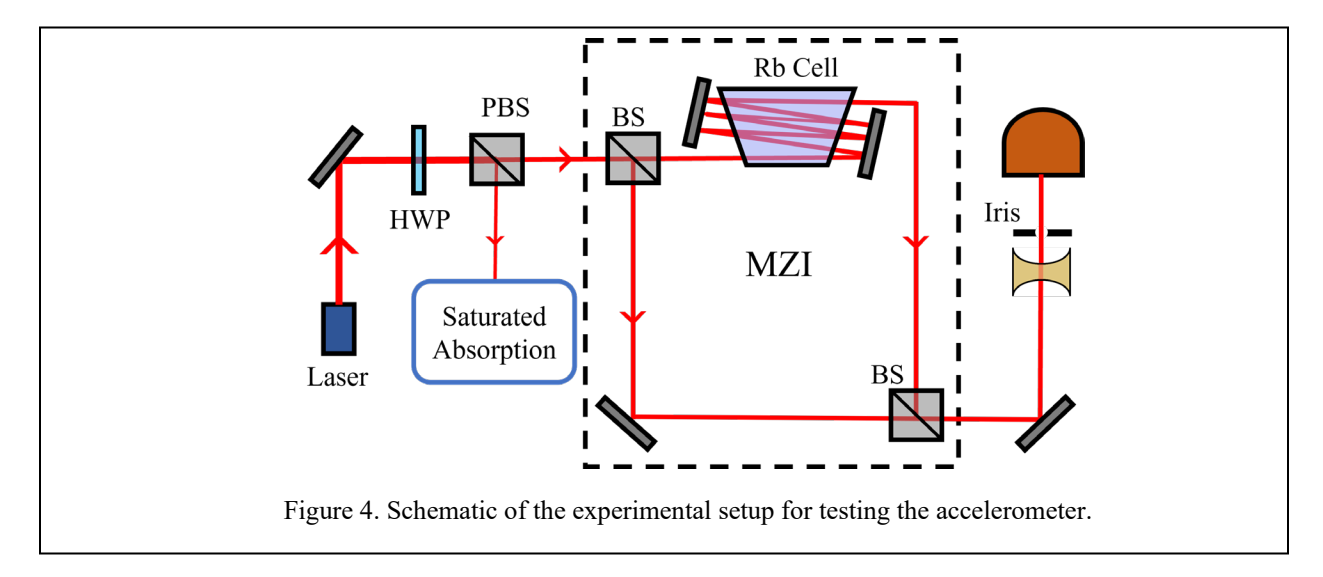
Raman laser has no effect on our result either, assuming Henry's model holds. Alternatively, the Raman lasers can be designed to operate superluminally, using any of the various approaches we have demonstrated so far [11,12,13,14,15,16]. In that case, the measurement sensitivity would be further enhanced by the superluminal laser enhancement factor [3,5].

3. Experiment

We have carried out experimental studies of the SLAUMZI, using two different mechanisms for generating the slow-light effect. In one case, we employed the positive group index that occurs when the laser is tuned between two absorption peaks, in the regime of linear absorption. In the other case, we made use of the coherent population trapping process.

a) Linear absorption case

The experimental configuration is illustrated schematically in Figure 4. The probe laser beam is first split into two parts. A small fraction is sent to a saturated absorption spectroscopy setup to record the nominal frequency of the laser. The majority of the laser power is sent into the unbalanced MZI. A Rb vapor cell, which contains a natural mixture of Rb, i.e. 72% ⁸⁵Rb and 28% ⁸⁷Rb, is placed in the upper arm of the unbalanced MZI. The windows of the Rb cell are wedged to prevent the etalon effect. The laser frequency is modulated by applying a voltage scan on the



controller and the voltage-frequency relation is determined by measuring the voltage difference corresponding to two absorption peaks in saturated absorption. Positive dispersion exists within the transparent region between the absorption peaks corresponding to the $5^2S_{1/2}$, F=2 to $5^2P_{1/2}$ transition and the $5^2S_{1/2}$, F=3 to $5^2P_{1/2}$ transition in 85 Rb, which is augmented by passing the probe multiple times through the cell. The temperature of the vapor cell is controlled by a PID (proportional-integral-differential) servo, and the degree of the slow-light effect is altered through setting the cell at different temperatures. A convex lens and an iris are placed in front of the photodetector so that the laser beam is expanded in the transverse plane and only the center of the interference pattern is detected.

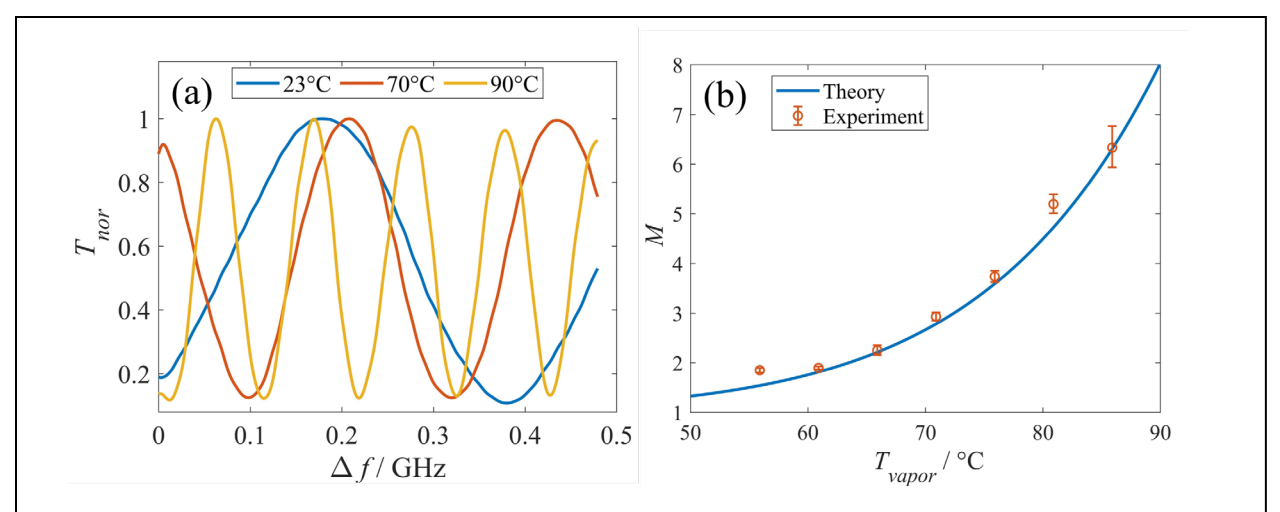


Figure 5. (a). Normalized transmission signal as functions of the laser frequency obtained by scanning the PZT length when the Rb cell temperature is measured as 23°C, 70°C and 90°C. (b). Calculated enhancement factor as a function of actual temperature of the Rb vapor in both experiment and theory. The temperature offset has been applied.

Figure 5(a) shows the normalized transmission signal from the MZI as functions of the laser frequency at different cell temperatures. At room temperature, the amount of absorption in the transparent region is negligible. As such, the blue curve can be considered as the non-dispersive result. Because of the length imbalance, the output signal changes with the laser frequency even without any dispersion in this case. By setting the group index $n_g = 1$ in Eq. (2) (non-dispersive case), we have $\Delta \Phi = \tau_{VAC} \Delta \omega$. Therefore, τ_{VAC} can be determined from the amount of frequency shift when the phase difference changes by 2π , which is found to be ~ 2.49 nsec. Given the length of the vapor cell, τ_0 and τ_D are determined to be 0.87 nsec and 1.61 nsec, respectively. The enhancement factor hence can be expressed as:

$$M_{fringe} = \frac{\Delta \omega_{nondispersive}}{\Delta \omega_{dispersive}} = \frac{\tau_{SL}}{\tau_{VAC}},$$
(25)

where $\Delta\omega$ is the change in the frequency that produces a phase difference of 2π . At highest cell temperature achieved in our experiments, the enhancement factor found to be ~6.33. According to Eq. (25), the slow light time delay is inferred as 15.76 nsec. Then the group index n_g can be determined from the expression $\tau_{SL} = \tau_0 + n_g \tau_D$, yielding a value of ~9.23.

Figure 5(b) shows the experimentally measured and theoretically predicted enhancement factor M as functions of the Rb cell temperature. The theoretical value of M as a function of temperature is calculated by using the N-level algorithm [31] and by considering all the Zeeman sublevels and including velocity averaging. Due to the difficulty in determining the actual temperature of the vapor inside the glass cell, we presume there is a constant temperature difference between the measured temperature and the actual value. Therefore, we vary the temperature difference in the simulation to find the best fitting to experimental results. As shown in the figure, the best fitting

occurs when the theoretical temperature, denoted as T_{vapor} , is 14.1°C lower than the measured value. At this temperature difference, the result shows consistency between the experimental and theoretical values.

The MMFS for this setup was also calculated. According to Eq.(24), as long as the laser linewidth is known, the ratio between the MMFSs of the SLAUMZI and the conventional technique can be determined if the same laser is used in the conventional technique. The laser linewidth was measured using the following process. We made use of two auxiliary lasers and mixed the output of three pairing of these three lasers. The beat signals were produced by a high-speed photodetector with a bandwidth of ~10 GHz. The output of the high-speed photodetector was sent to a spectrum analyzer, and the spectral widths of the three beat signals were measured individually. This gives three equations with three unknown laser linewidths. By solving the equations, the spectral width of each of the three lasers could be determined. Using this approach, the linewidth of the probe laser [Toptica DL-Pro; 12 mW] for the SLAUMZI apparatus was determined to be ~301.5 kHz at $P_{out} = 0.5$ mW . At the condition where the highest M is obtained, from Eq.(24), the ratio between the MMFSs can be written as (using $\sigma \approx 1$):

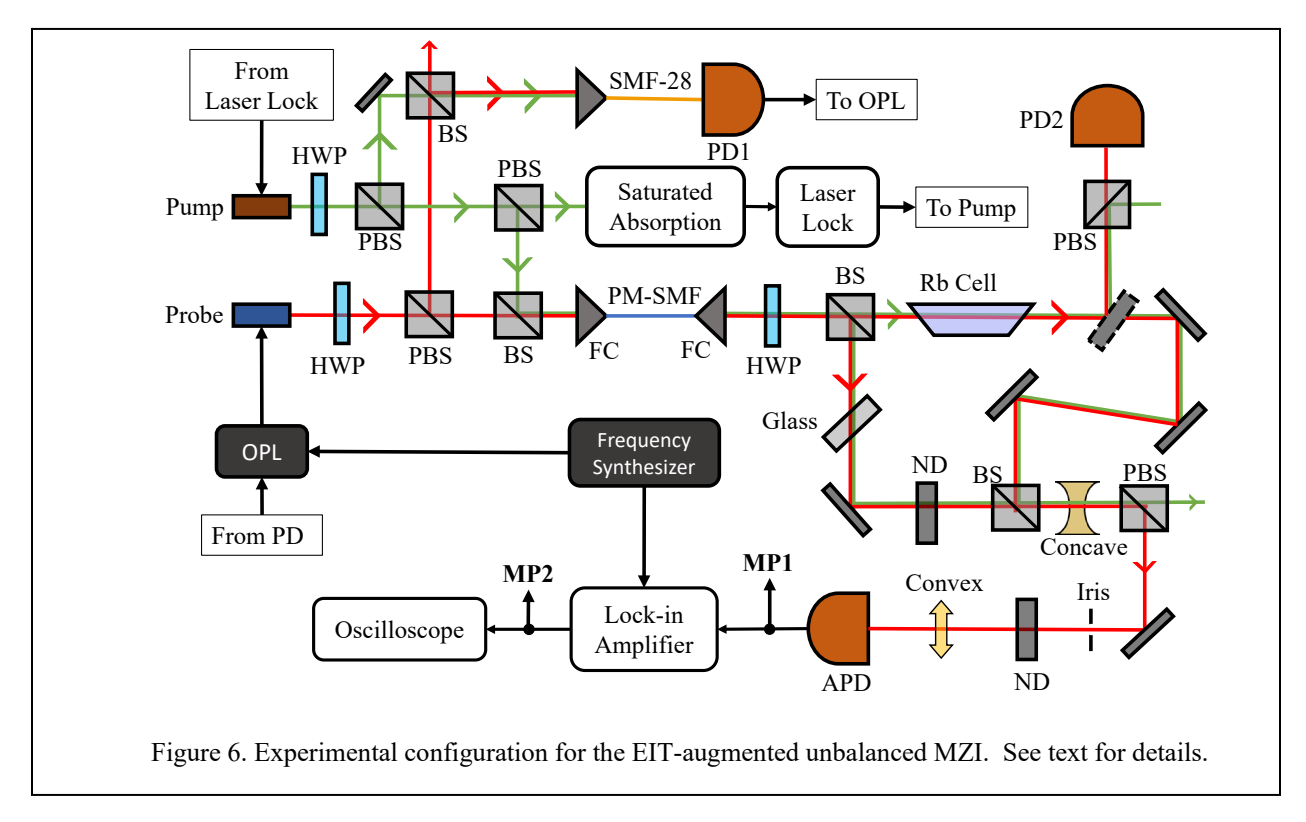
$$\frac{\delta\omega_{STD}}{\delta\omega_{SLAUMZI}} = \frac{e^{0.25}}{\sqrt{2}} \sqrt{\frac{N}{\tau_L}} \tau_{SL} = \frac{e^{0.25}\tau_{SL}}{\sqrt{2}} \sqrt{\frac{P_{fringe}}{\tau_L \hbar \omega}} \approx 313,$$
 (26)

where $\hbar\omega$ and $P_{fringe}=0.39$ mW are the single photon energy and the laser power at which the interference fringe is recorded, respectively. Thus, using the modest dispersion produced in the linear absorption regime, the SLAUMZI apparatus is expected to improve the MMFS by a factor of ~313 compared to a conventional-laser-based frequency measurement.

b) The EIT case

Electromagnetic Induced Transparency (EIT) is a two-photon process that can produce the group index as large as 10⁶ [29,30]. By co-propagating two laser beams through a Rb vapor cell with crossed polarizations, both lasers see a greatly reduced absorption when the frequency difference between the two lasers corresponds to the hyperfine splitting in the ground state. This induced transparency is attributed to the formation of a dark state. Figure 6 shows the complete setup of the EIT-enhanced unbalanced MZI (UMZI). Two lasers, for the sake of distinction, are named as "probe" and "pump", respectively and are locked by an offset phase lock (OPL) at the frequency difference of the hyperfine states $5S_{1/2}$ F = 2 and $5S_{1/2}$ F = 3, i.e. 3.0357 GHz. The OPL takes two inputs, which are the beating signal from the fiber-coupled photodetector (PD1) and the radio frequency from the frequency synthesizer, and the feedback signal is applied to the probe laser controller. At the same time, the pump laser is separately locked to the optical transition $5S_{1/2}$ F = 2 to $5P_{1/2}$ F' = 3 via saturated absorption spectroscopy. A polarization-maintaining single mode fiber (PM-SMF) is used for mode matching of the two lasers. The EIT signal is detected by directing the beam out to the photodetector (PD2) using a foldable mirror (dashed in the figure), while a polarizing beam splitter (PBS) filters out the pump beam. On the lower arm of the UMZI, a glass plate is inserted and its position can be slightly adjusted by a PZT-driven holder, which is able to add more than π of phase difference between the two arms. To measure the EIT

signal, the frequency of the probe laser is swept around the center frequency. A typical EIT signal observed is shown in Figure 7, with a linewidth of ~ 2.77 MHz.



To characterize the fringe magnification due the EIT process, we apply a square wave modulation at 200 kHz (which is much less than the EIT linewidth) to the OPL, which causes the frequency of the probe beam to be modulated. We adjust the glass plate until the amplitude of the modulation observed at the APD is maximized, corresponding to operating at a point on the fringe with the maximum slope. The amplitude of the modulation is measured twice: once in the presence of the EIT effect, and once when the EIT process is turned off (e.g., by tuning the probe frequency far away from any resonance, and blocking the pump beam from entering the vapor cell inside the UMZI). The case when no EIT effect is present is when the group index is unity.

The enhancement factor can be expressed as:

$$M = \frac{\left(\Delta V_{pp}^{\text{max}}\right)_{EIT}}{\left(\Delta V_{pp}^{\text{max}}\right)_{STD}} \tag{27}$$

where $\left(\Delta V_{pp}^{\text{max}}\right)_{EIT}$ and $\left(\Delta V_{pp}^{\text{max}}\right)_{STD}$ are the maximized peak-peak value in the EIT and non-EIT case, respectively. The enhancement factor determined from the experiment, based on Eq. (27), is ~257. Given the length of the Rb cell and Eq.(3), the group index is calculated to be 1759. An approximate fitting of the data via numerical modeling yields a value of ~1752, in close agreement with the measurement.

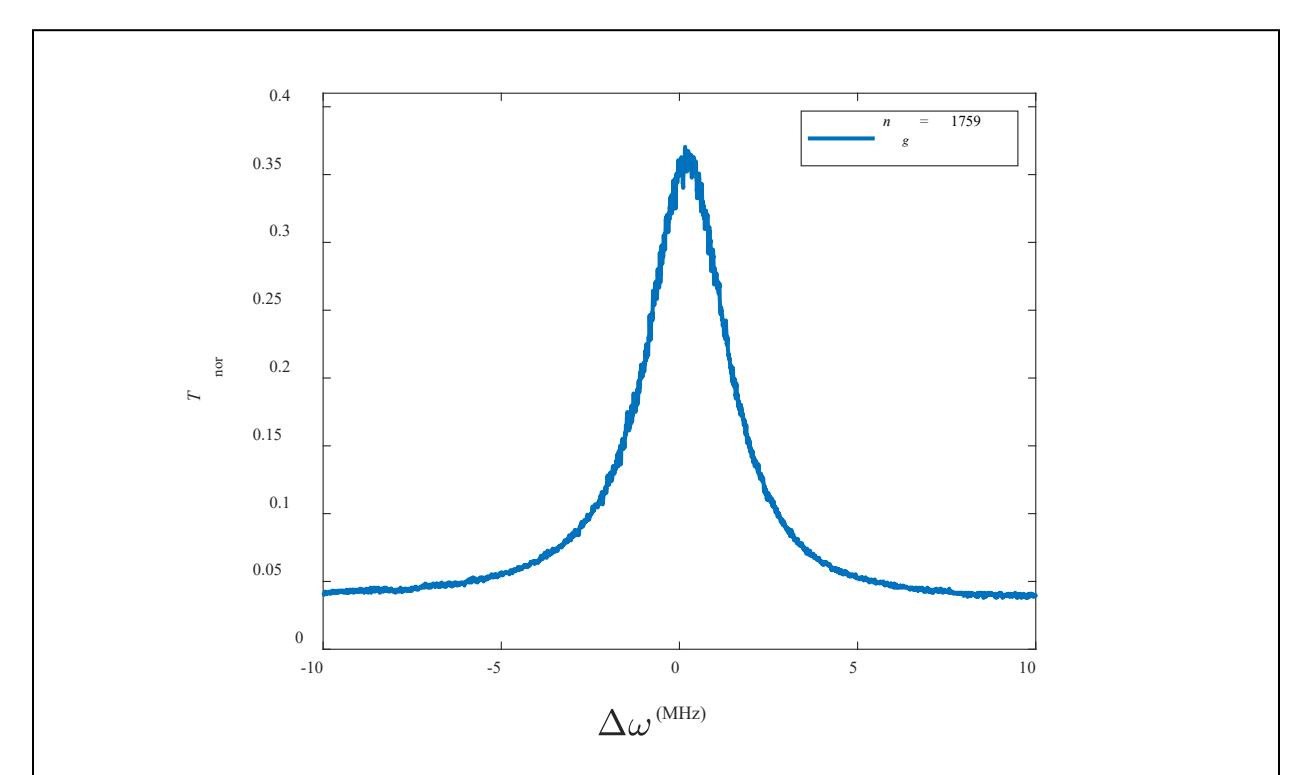


Figure 7. A typical EIT signal observed, where the linewidth is ~2.77 MHz. The horizontal axis represents the frequency deviation from the center frequency $\omega_c = 3.0357584 \text{GHz}$ and the vertical axis denotes the normalized transmission. The signal is averaged using 32 frames in the oscilloscope.

The probe laser has a linewidth of 301.5 kHz at $P_{out} = 0.5$ mW. Therefore, the enhancement in the MMFS is found to be:

$$R = \frac{\delta \omega_{STD}}{\delta \omega_{SLAUMZI}^{EIT}} = \frac{e^{0.25}}{\sqrt{2}} \sqrt{\frac{\sigma N}{\tau_L}} \tau_{SL}^{EIT} = \frac{e^{0.25} \tau_{SL}^{EIT}}{\sqrt{2}} \sqrt{\frac{\sigma P_{fringe}^{EIT}}{\tau_L \hbar \omega}} \approx 22355$$
 (28)

where $P_{\text{fringe}}^{EIT} = 0.80 \text{mW}$ is the power of the probe laser and $\tau_{\text{SL}}^{EIT} = 2957.6 n \text{sec}$ is the slow-light time delay and $\sigma = 0.41$. This result implies that the SLAUMZI is able to measure a frequency shift that is a factor of around $2*10^4$ smaller than what can be achieved using the standard technique.

When comparing the MMFS for the standard technique with that of the SLAUMZI technique, we have assumed that the quantum efficiency (η) of the detector in both cases would be the same. For the APD used the SLAUMZI output, we have $\eta \simeq 0.5$. The measurement bandwidth, $\Gamma_{_M}/2\pi$, is given by the bandwidth of the APD, which is ~50 MHz. We also know that the linewidth of the laser, $\Gamma_{_L}/2\pi$ is ~301.5 kHz. As such, according to Eq.(23), the MMFS for the standard technique would be:

$$\Delta f_{MIN}^{STD} = \Delta \omega_{MIN}^{STD} / 2\pi = \sqrt{\frac{\Gamma_L \Gamma_M}{\eta 4\pi^2}} = \sqrt{\frac{50*10^6*301.5*10^3}{0.5}} \simeq 5.49*10^6 \ Hz$$
 (29)

Given the enhancement factor estimated above to be ~22355, we would then expect that the MMFS for the SLAUMZI would be:

$$\Delta f_{SLAUMZI}^{EIT} = \Delta \omega_{SLAUMZI}^{EIT} / 2\pi = \sqrt{\frac{\Gamma_L \Gamma_M}{\eta 4\pi^2}} \simeq \frac{5.49 * 10^6 \text{ Hz}}{22355} \simeq 246 \text{ Hz}$$
 (30)

We measured the MMFS for the SLAUMZI using a variation of the technique use for measuring the fringe magnification factor. Specifically, the probe frequency was modulated around the frequency corresponding the peak of the EIT signal, using a square wave. The glass plate was adjusted to maximize the signal modulation observed by the APD at the output port., thus ensuring operation at the point where the slope of the fringe is maximum. The APD signal was then fed into a lock-in-amplifier (LIA) synchronized with modulating signal, and demodulated after optimizing its phase. A non-zero value of the output of the LIA indicates detection of modulation of the laser frequency. The swing in laser frequency, denoted as ω_m , due to the application of the square wave modulation, was varied while observing the LIA output. The scaling of ω_m was calibrated separately by applying a ramp voltage and observing saturated absorption peaks with known separations.

Figure 8 shows the output of the LIA, denoted as V_{LiA} , as a function of the frequency swing, ω_m . To model the system, we assume an ideal LIA output without any noise as:

$$V_{ideal} = k \frac{\omega_m}{2\pi} \tag{31}$$

where V is the LIA output, and k is the coefficient which can be obtained by fitting the linear part of the experimental data. The effect of noise is modeled as a constant in the LIA output and is set to be a variable which can be changed to give the best fitting result. If we denote the noise as V_N , the total output can be written as:

$$V_{ft} = k \frac{\omega_m}{2\pi} + V_N \tag{32}$$

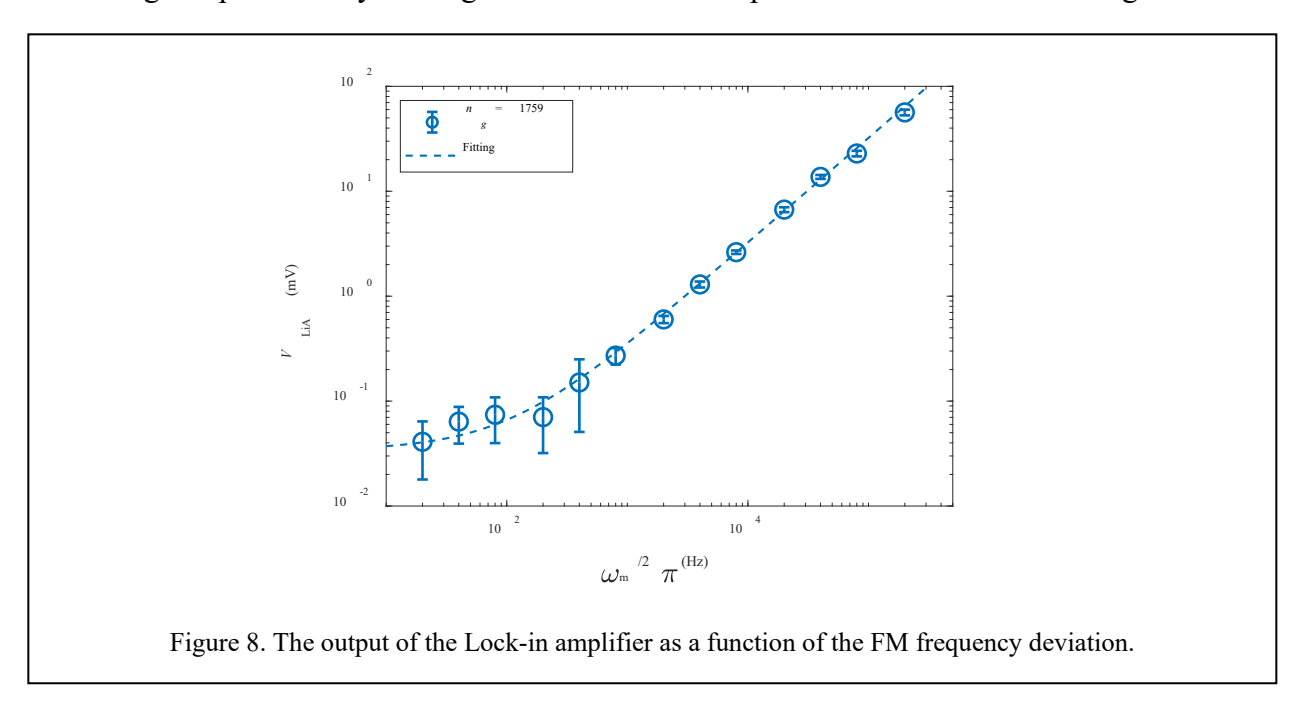
Therefore, corresponding to each frequency deviation ω_m in the experiment, the difference between the fitting value and experimental value can be defined as:

$$\Delta V_{diff}\left(\omega_{m}\right) \equiv V_{LiA}\left(\omega_{m}\right) - V_{ft}\left(\omega_{m}\right) = V_{LiA}\left(\omega_{m}\right) - \left(k\frac{\omega_{m}}{2\pi} + V_{N}\right)$$
(33)

Here we further define the sum of the square of the difference as K_{sum} , which is written as:

$$K_{sum} = \sum_{m} \left(\Delta V_{diff} \left(\omega_{m} \right) \right)^{2} = \sum_{m} \left(V_{LiA} \left(\omega_{m} \right) - k \frac{\omega_{m}}{2\pi} - V_{N} \right)^{2}$$
(34)

The fitting is optimized by finding the V_N which corresponds to minimized K_{sum} . Figure 8 also



shows the fitting curve found by implementing the process described above. The MMFS is then defined, rather arbitrarily, as the frequency at which the ideal signal equals to the noise level, which can be expressed as:

$$V_{ideal} = V_{N} \tag{35}$$

Applying this criterion, we get the MMFS for the SLAUMZI system to be

$$\Delta f_{SLAUMZI}^{EIT} = \Delta \omega_{SLAUMZI}^{EIT} / 2\pi = V_N / k \approx 104 Hz$$
 (36)

which is reasonably close to the value estimated under Eq. (30), given the rather arbitrary criterion we have employed regarding the experimentally determined MMFS.

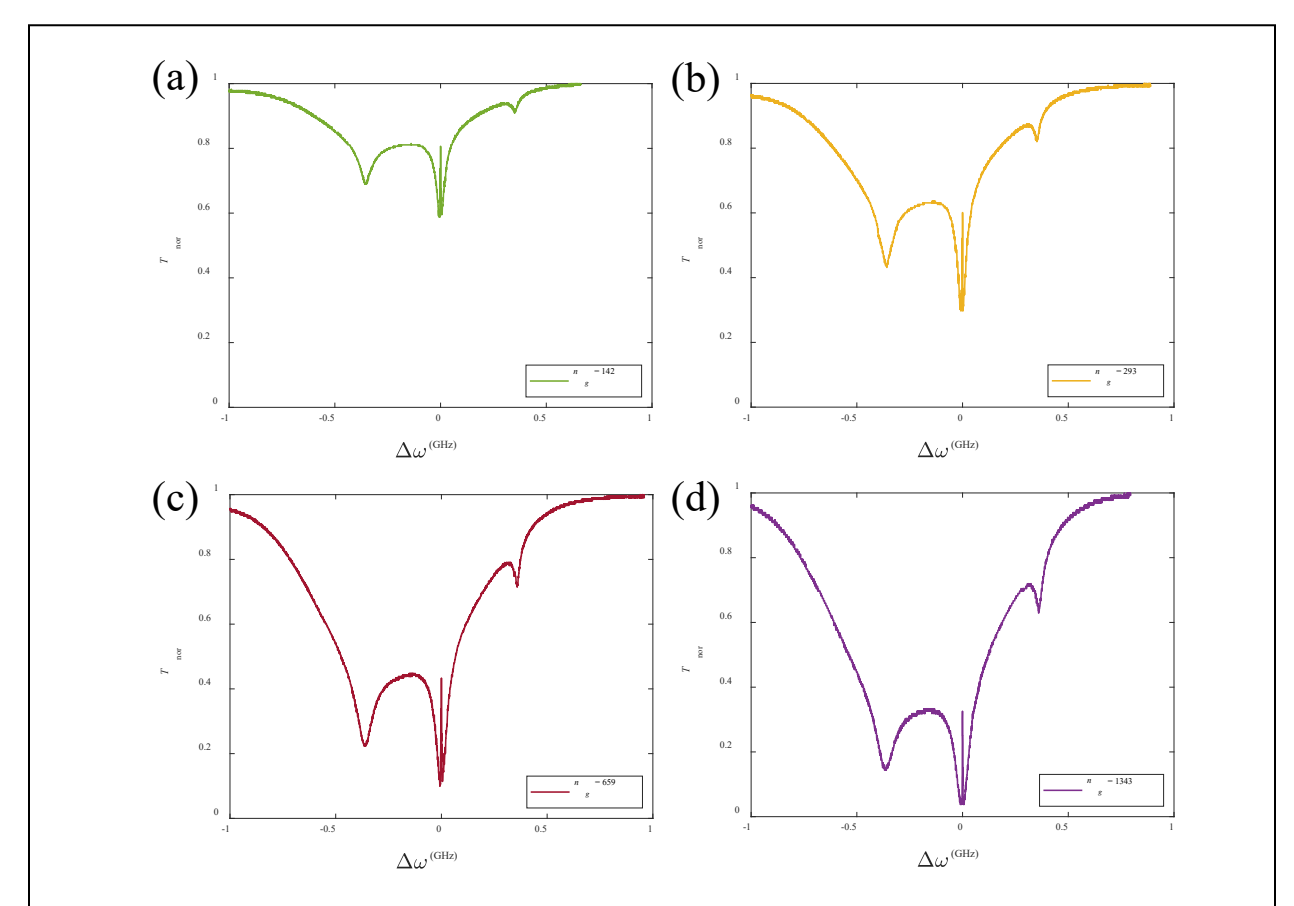
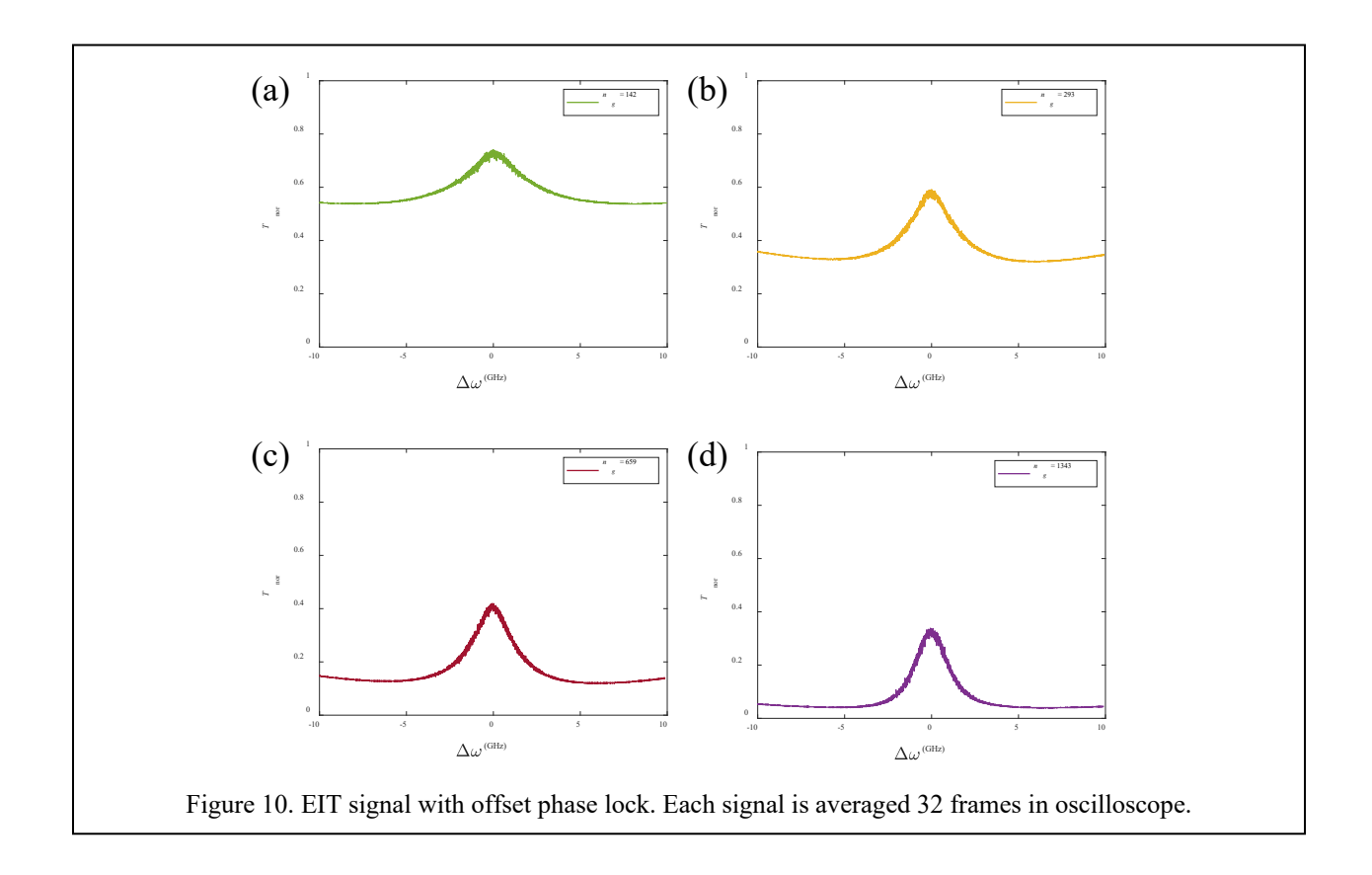


Figure 9. EIT signal at different group indices. The horizontal axis represents the frequency deviation from the center of the EIT signal and the vertical axis is the normalized transmission.

To confirm the validity of our interpretation of the MMFS, more experiments have been done at different group indices, which were varied by changing the Rb cell temperature and optical powers. Figure 9 shows the EIT signal at a larger scale without offset phase locking the probe laser, where group index is determined to be 142, 293, 659 and 1343 for the four cases by using the technique described before.

EIT signals with higher spectral resolution can be obtained by offset phase locking the probe to the pump and scanning the probe frequency over a small range around the center frequency, which corresponds to the ground state frequency difference, i.e., ~3.0357584 GHz. The exact center frequency is found by fine tuning the offset frequency between the probe and the pump to maximize the transmission signal after the Rb cell. Figure 10 shows the higher resolution EIT signals when the probe is offset phase locked to the pump, for the four cases shown in Figure 9.



With the knowledge of group index, the magnification factor M is calculated by Eq. (3) to be 22, 43, 97 and 196 respectively. Considering the input power $P_{fringe}^{EIT} = 0.60 \text{mW}$ at all group indices, except at $n_g = 1343$, where $P_{fringe}^{EIT} = 0.80 \text{mW}$, the enhancement factor for the MMFS are found to be:

$$R(n_g = 142) = \frac{e^{0.25} \tau_{SL1}^{EIT}}{\sqrt{2}} \sqrt{\frac{\sigma_1 P_{fringe}^{EIT}}{\tau_L \hbar \omega}} \approx 2115$$

$$R(n_g = 293) = \frac{e^{0.25} \tau_{SL2}^{EIT}}{\sqrt{2}} \sqrt{\frac{\sigma_2 P_{fringe}^{EIT}}{\tau_L \hbar \omega}} \approx 3748$$

$$R(n_g = 659) = \frac{e^{0.25} \tau_{SL3}^{EIT}}{\sqrt{2}} \sqrt{\frac{\sigma_3 P_{fringe}^{EIT}}{\tau_L \hbar \omega}} \approx 7092$$

$$R(n_g = 1343) = \frac{e^{0.25} \tau_{SL4}^{EIT}}{\sqrt{2}} \sqrt{\frac{\sigma_4 P_{fringe}^{EIT}}{\tau_L \hbar \omega}} \approx 14612$$

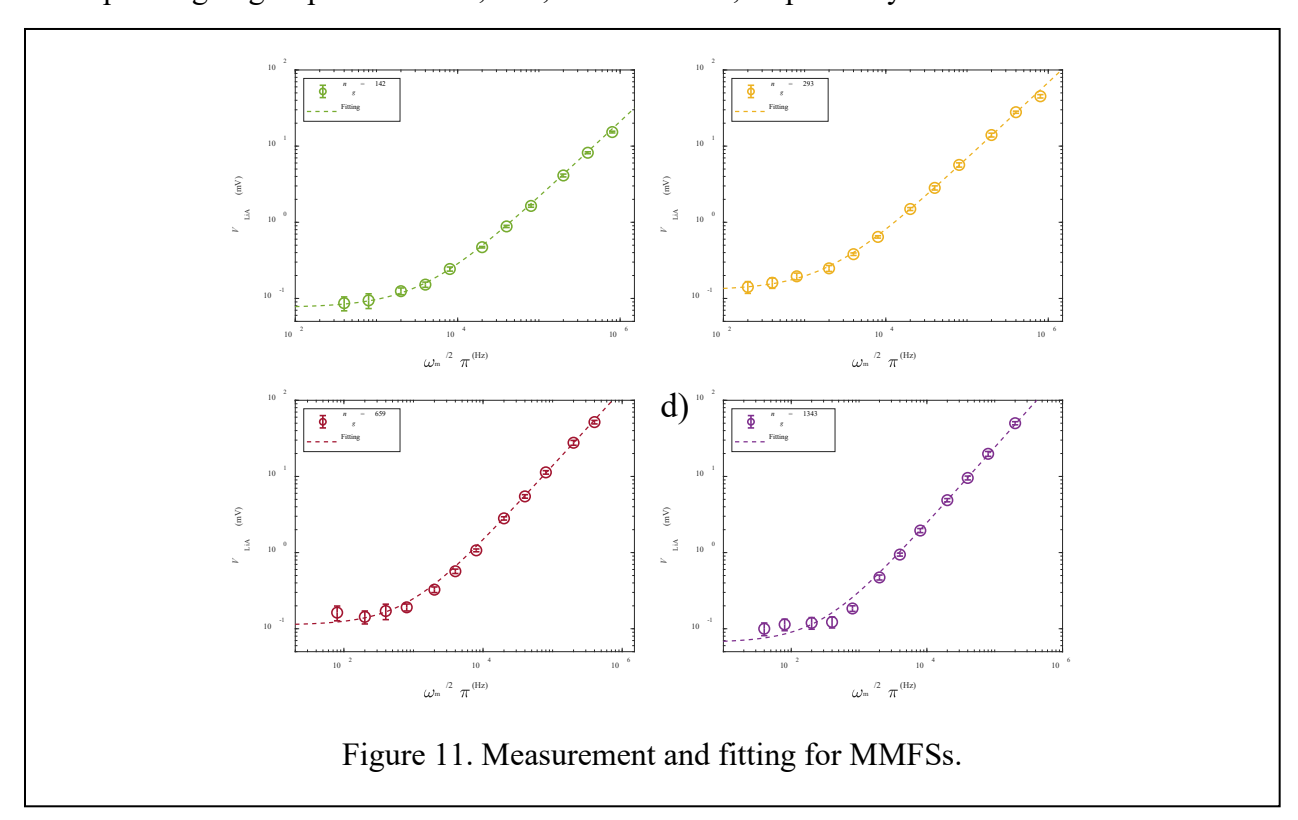
where $\tau_{SL1}^{EIT}=39.4n\sec$, $\tau_{SL2}^{EIT}=79.7n\sec$, $\tau_{SL3}^{EIT}=177.2n\sec$ and $\tau_{SL4}^{EIT}=360.0n\sec$ are the slow light time delays and $\sigma_1=0.78$, $\sigma_2=0.6$, $\sigma_3=0.42$ and $\sigma_4=0.33$ are the normalized

transmission at the center frequency for each group index, respectively. Given the ratio of MMFS, the theoretical MMFS can be calculated as:

$$MMFS(n_g = 142) = 2596Hz$$
 $MMFS(n_g = 293) = 1465Hz$
 $MMFS(n_g = 659) = 775Hz$
 $MMFS(n_g = 1343) = 376Hz$

(38)

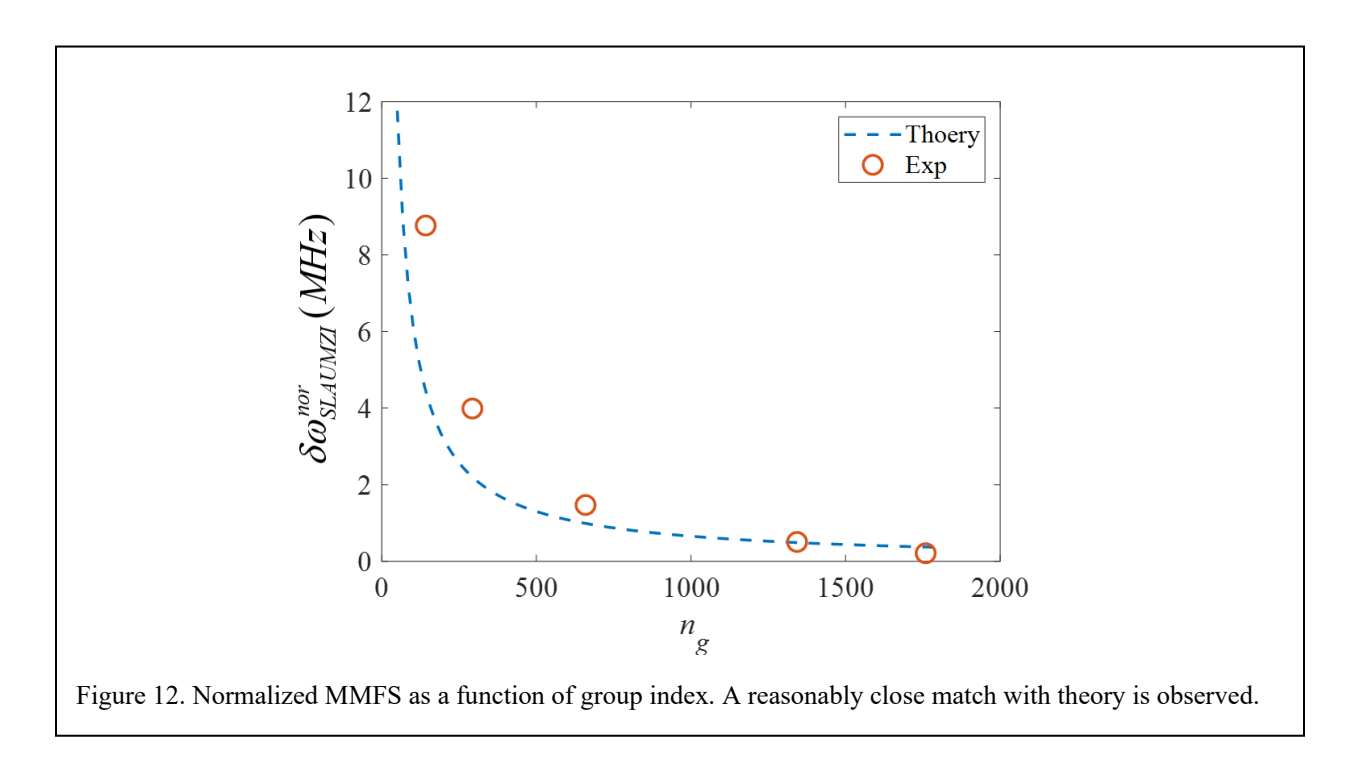
By plotting the LIA output as a function of the frequency deviation, the actual MMFS can be obtained through fitting the experiment data and finding the frequency at which the ideal LIA output equals noise. Figure 11 shows the measurement at different cell temperatures along with the best fitting curves. The MMFSs are found to be 3621Hz, 1878Hz, 813Hz and 275Hz corresponding to group indices 142, 293, 659 and 1343, respectively.



From Eq. (15), it is obvious that $\delta\omega_{SLAUMZI}$ varies as a function of the transmitted powers of the EIT signal, which is correlated with the group index. This interdependence is hard to model by a simple formula. Therefore, it is useful to define a normalized MMFS as

$$\delta\omega_{SLAUMZI}^{nor} = \sqrt{\sigma N \tau_m} \delta\omega_{SLAUMZI} = \frac{\sqrt{2}}{e^{0.25} \tau_{SL}} = \frac{\sqrt{2}}{e^{0.25} M \tau_{VAC}}$$
(39)

where σ is the transmission at the EIT peak, N is the number of photons received by the APD per unit time, τ_m is the measurement time of the APD, τ_{SL} is the time delay of slow light media, M is the fringe magnification factor and τ_{VAC} is the time delay in the unity group index case. For any



specific MMFS obtained experimentally, $\delta\omega_{SLAUMZI}^{nor}$ can be easily calculated and compared with the theoretical value. Figure 12 shows such a comparison by using the MMFSs obtained in the experiment. It can be observed that experimental results follow the theoretical value closely.

4. Conclusions

We have demonstrate a slow-light augmented unbalanced Mach-Zehnder interferometer (MZI) which can be used to enhance very significantly the sensitivity of measuring the frequency shift in a laser. We have shown theoretically and verified experimentally that the degree of enhancement depends on the group index of the slow-light medium, the degree of imbalance between the physical lengths of the two arms of the MZI, and the spectral width of the laser. For a laser based on a high-finesse cavity, yielding a narrow quantum noise limited spectral width, the group index has to be larger than the finesse in order to achieve enhancement in measurement sensitivity. For the reported results, strong slow-light effect was produced by employing electro-magnetically induced transparency via coherent population trapping in a buffer-gas loaded vapor cell of Rb atoms, with a maximum group index of ~1759. The observed enhancement in sensitivity for a range of group indices agrees well with the theoretical model. The maximum enhancement factor observed is ~22355, and much larger values can be obtained using cold atoms for producing the

slow-light effect, for example. We have also shown a specific architecture for enhancing the sensitivity of a gyroscope and accelerometer using bi-directional and non-degenerate Raman lasers employing the slow-light augmented unbalanced MZI. The Raman lasers can be either subluminal or superluminal. In the case when the Ramn lasers are superluminal, the sensitivity would be increased further due to the superluminal enhancement effect. More generally, the sensitivity of any sensor that relies on measuring the frequency shift of a laser can be enhanced substantially using this technique. These include, but are not limited to, gyroscopes and accelerometers based on a conventional ring laser or a superluminal ring laser, and detectors for virialized ultra-light field dark matter. We also show how similar enhancements can be achieved in a slow-light augmented unbalanced Michelson interferometer.

Reference

[1]E. J. Post, "The Sagnac Effect," Rev. Mod. Phys. 39, 475 (1967)

[2] W. W. Chow, J. Gea-Banacloche, L. M. Pedrotti, V. E. Sanders, W. Schleich, and M. O. Scully, "The ring laser gyro," Reviews of Modern Physics 57, 61 (1987)

[3] M. S. Shahriar, G. S. Pati, R. Tripathi, V. Gopal, and M. Messall, "Ultrahigh enhancement in absolute and relative rotation sensing using fast and slow light," Phys. Rev. A 75, 053807-1 - 053807-10 (2007).

[4] A. A. Geraci, C. Bradley, D. Gao, J. Weinstein, and A. Derevianko, "Searching for Ultralight Dark Matter with Optical Cavities," Phys. Rev. Lett. 123, 031304 (2019).

[5] H. N. Yum, M. Salit, J. Yablon, K. Salit, Y. Wang, and M. S. Shahriar, "Superluminal ring laser for hypersensitive sensing," Opt. Express 18(17), 17658 (2010).

[6] J. Scheuer and S.M. Shahriar, "Lasing dynamics of super and sub luminal lasers", Opt. Express 23, 32350–32365 (2015)

[7] Y. Wang, Z. Zhou, J. Yablon, and M. S. Shahriar, "Effect of Multi-Order Harmonics in a Double-Raman Pumped Gain Medium for a Superluminal Laser," Opt. Eng. 54(5), 057106 (2015).

[8] J. Yablon, Z. Zhou, M. Zhou, Y. Wang, S. Tseng, and S.M. Shahriar, "Theoretical modeling and experimental demonstration of Raman probe induced spectral dip for realizing a superluminal laser," Optics Express, Vol. 24, No. 24, 27446 (2016)

[9] M. Zhou, Z. Zhou, M. Fouda, N.J. Condon, J. Scheuer, and M.S. Shahriar, "Fast-light Enhanced Brillouin Laser Based Active Fiber Optic Sensor for Simultaneous Measurement of Rotation and Strain," Journal of Lightwave Technology, 35 (23), 5222 (2017).

[10] M.F. Fouda, M. Zhou, H.N. Yum, and S.M. Shahriar, "Effect of cascaded Brillouin lasing due to resonant pumps in a superluminal fiber ring laser gyroscope," Opt. Eng. 57(10), 107108 (2018)

[11] Z. Zhou, M. Zhou and S.M. Shahriar, "A superluminal Raman laser with enhanced cavity length sensitivity," Optics Express 27, 29739-29745 (2019)

[12] Y. Sternfeld, Z. Zhou, J. Scheuer, and M. S. Shahriar, "Electromagnetically induced transparency in Raman gain for realizing a superluminal ring laser," Opt. Express 29, 1125-1139 (2021).

[13] Zifan Zhou, Nicholas Condon, Devin Hileman, and M. S. Shahriar, "Observation of a highly superluminal laser employing optically pumped Raman gain and depletion," Opt. Express 30, 6746-6754 (2022).

[14] Z. Zhou, R. Zhu, N. Condon, D. Hileman, J. Bonacum and S.M. Shahriar, "Bi-directional Superluminal Ring Lasers without Cross-talk and Gain Competition," Appl. Phys. Lett. 120, 251105 (2022)

[15] Z. Zhou, R. Zhu, Y. Sternfeld, J. Scheuer, J. Bonacum, and S. M. Shahriar, "Demonstration of a Superluminal Laser using Electromagnetically Induced Transparency in Raman Gain," Opt. Express 31(9), 14377-14388 (2023)

[16] Y. Sternfeld, Z. Zhou, S.M. Shahriar and J. Scheuer, "Single-pumped gain profile for a superluminal ring laser," Optics Express 31(22) 36952-36965 (2023)

[17] Z. Shi, Robert, W. Boyd, Daniel J. Gauthier, and C. C. Dudley, "Enhancing the spectral sensitivity of interferometers using slow-light media," Opt. Lett. 32, 915-917 (2007).

[18] C.H. Townes, "Some applications of optical and infrared masers," in *Advances in Quantum Electronics*, J.R. Singer., Ed., New York: Columbia Univ. Press, 1961, pp 1-11.

- [19] C. H. Henry, "Theory of the Linewidth of Semiconductor Lasers," IEEE J. Of Quantum Electronics, Vol. QE-18, No. 2, (1982)
- [20] T.A. Dorschner, H.A. Haus, M. Holz, I.W. Smith, H. Statz, "Laser gyro at quantum limit", IEEE J. Quant. Elect. QE-16, 1376 (1980)
- [21] B. T. King, "Application of superresolution techniques to RLGs: exploring the quantum limit," Applied Optics **39**, 6151 (2000).
- [22] M. O. Scully and M.S. Zubairy, Quantum Optics, Cambridge University Press (1997).
- [23] F. Aronowitz, in Laser Applications, edited by M. Ross (Academic, New York) pp. 113-200.
- [24] J. Yablon, Z. Zhou, N. J. Condon, D. J. Hileman, S. C. Tseng, and M.S. Shahriar, "Demonstration of a highly subluminal laser with suppression of cavity length sensitivity by nearly three orders of magnitude." Optics Express, 25 (24), 30327 (2017).
- [25] W. M. Itano, J. C. Bergquist, J. J. Bollinger, J. M. Gilligan, D. J. Heinzen, F. L. Moore, and D. J. Wineland, "Quantum projection noise: Population fluctuations in two-level systems," Phys. Rev. A 47, 3554 (1993).
- [26] In order to account for the effect of the absorption from a phase insensitive process, as well as the sub-unity quantum efficiency of a intensity-measuring detector, one can formulate an equivalent ideal beamsplitter for each case, where the degree of attenuation is accounted for by the finite transmittivity of the beam splitter, and a vacuum mode is added at the free port in order to ensure that the output satisfies the Bosonic commutation relations [27,28]. However, when the input fields being attenuated are much stronger than the vacuum mode, the result would become essentially equivalent to the simple model we have used here [28].
- [27] C.M. Caves, "Quantum limits on noise in linear amplifiers," Phys. Rev. D 26, 8, 1817 (1982).
- [28] B.L. Schumaker, "Noise in Homodyne Detection," Optics Letters, Vol 9, No. 5, 189 (1984)
- [29]L.V. Hau, S. E. Harris, Z. Dutton and C. H. Behrooz, "Light speed reduction to 17 metres per second in an ultracold atomic gas," Nature 397, 18 (1999).
- [30]A. V. Turukhin, V.S. Sudarshanam, M.S. Shahriar, J.A. Musser, B.S. Ham, and P.R. Hemmer, "Observation of Ultraslow and Stored Light Pulses in a Solid," Phys. Rev. Lett. 88, 023602 (2001)
- [31] M. S. Shahriar, Ye Wang, S. Krishnamurthy, Y. Tu, G.S. Pati, and S. Tseng, "Evolution of an N-level system via automated vectorization of the Liouville equations and application to optically controlled polarization rotation," Journal of Modern Optics, 61:4, 351-367 (2014).